Electronic Appendix

In this appendix we report all modelling assumptions, mathematical details, numerical approximations, and relevant references used in our analysis. Some statements and formulas presented in the paper are repeated here in order to obtain a self-contained presentation of our analysis that could be read without going back and forth between the paper and the appendix. Equations are numbered as (A1), (A2),... and when they correspond to a specific equation mentioned in the paper, this is explicitly pointed out.

A1 The ecological model

The ecological community we consider is a predator-prey interaction described by the standard Rosenzweig-Mac Arthur model (Rosenzweig and MacArthur, 1963)

$$\dot{x}(t) = x(t)\left[r\left(1-\frac{x(t)}{K}\right) - \frac{ay(t)}{h+x(t)}\right] \tag{A1}$$

$$\dot{y}(t) = y(t)\left[b + e\frac{ax(t)}{h+x(t)} - d\right] \tag{A2}$$

(eqs. (3) and (4) in paper), where $x(t)$ and $y(t)$ are prey and predator population densities at time t. In the absence of predator, the prey population grows logistically (with intrinsic growth rate r and carrying capacity K), while, in the absence of prey, the predator population decays exponentially (we assume that the intrinsic birth rate b is smaller than the death rate d but that the maximum birth rate $(b+ea)$ is greater than d). Moreover, predators have a Holling type II functional response (with maximum predation rate a and half-saturation constant h) and extra natality resulting from predation is simply proportional to the predation rate through an efficiency coefficient e.

For any parameter setting, model (A1, A2) has a global attractor in the positive quadrant. If the prey carrying capacity is low, i.e.

$$K < \frac{h(d-b)}{ea-d+b} \tag{A3}$$

the attractor is the equilibrium $(K,0)$, i.e. the predator population goes extinct. In contrast, if the prey carrying capacity is such that

$$\frac{h(d-b)}{ea-d+b} < K < \frac{h(ea+d-b)}{ea-d+b} \tag{A4}$$

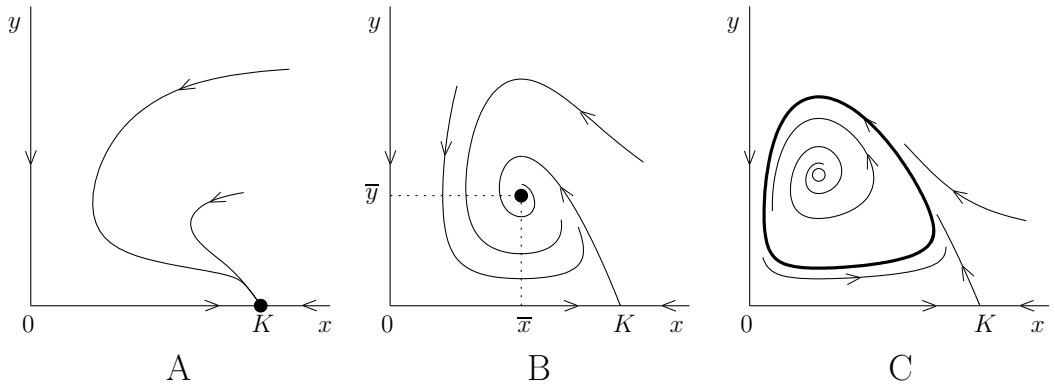

Figure A1: The three state portraits of model (A1, A2): A, predator extinction (see eq. (A3)); B, stationary coexistence (see eq. (A4)); C, cyclic coexistence (see eq. (A6)).

stationary coexistence occurs at the equilibrium

$$\bar{x} = \frac{h(d-b)}{ea-d+b} \qquad \bar{y} = \frac{r}{a}\left(1-\frac{\bar{x}}{K}\right)(h+\bar{x}) \tag{A5}$$

while for high values of K, i.e.

$$K > \frac{h(ea+d-b)}{ea-d+b} \tag{A6}$$

populations coexist on a limit cycle, as shown in Fig. A1. When eq. (A6) is satisfied with the equality sign, i.e. when the vertical predator isocline ($x = (d-b)h/(b+ea-d)$) is passing through the vertex of the non-trivial prey isocline (the parabola $y = r/a\,(1-x/K)\,(h+x)$, see Fig. A2), the equilibrium $(\bar{x}, \bar{y})$ given by eq. (A5) is critically stable and the populations are balanced between stationary and cyclic coexistence. The limit cycle is not known analytically, and this implies that the evolutionary dynamics can not be described explicitly when the prey carrying capacity is high.

A2 The case of slow predator and fast prey

If prey grow at a much faster rate than predators, the limit cycle can be fairly well approximated by the so-called singular limit cycle, which can be easily derived from the isoclines, as shown in Fig. A2. The singular cycle is composed of two fast and two slow phases. The first fast motion is the collapse of the prey population: it occurs when the predator abundance is at its highest value $y_{\max}$. Then, in the absence of prey, predator abundance slowly decays from $y_{\max}$ until a lower threshold $y_{\min}$ is reached. At this point, the prey population rises quickly to $x_{\max}$ while predator abundance remains at its lowest value. Finally, the second slow motion takes place: the predator slowly regenerates and the prey slowly decays along the non-trivial

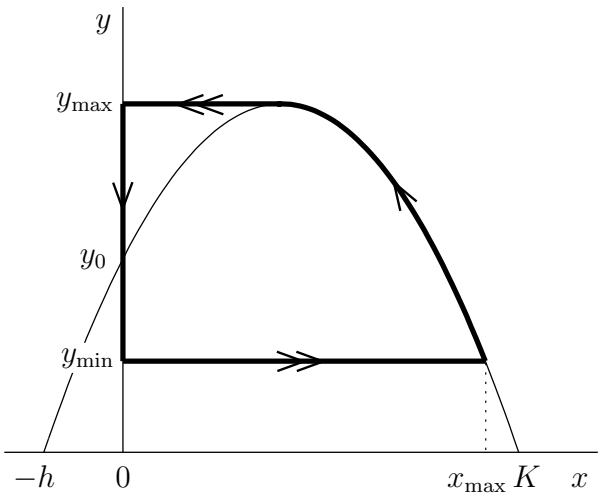

Figure A2: Non-trivial prey isocline (parabola) and singular limit cycle; single [double] arrows indicate slow [fast] motion.

prey isocline (the parabola in the figure).

The maximum predator abundance $y_{\max}$ (the y coordinate of the vertex of the parabola) is given by

$$y_{\max} = \frac{r(K+h)^2}{4aK} \tag{A7}$$

while it can be shown (Rinaldi and Muratori, 1992) that the minimum predator abundance $y_{\min}$ is the solution of the following transcendental equation

$$y_{\max} - y_{\min} = y_0 \log \frac{y_{\max}}{y_{\min}} \tag{A8}$$

where $y_0 = hr/a$ is the intersection of the prey isocline with the vertical axis (see Fig. A2).

A3 Dependence of demographic parameters upon adaptive traits

We now denote by u for the prey, and v for the predator, two species-specific adaptive traits which control the predator-prey interactions. We assume that the prey has density- and trait-independent birth rate, while its death rate has a density-dependent component controlled by u. Thus, r is constant while K depends on u. We further assume that K peaks at u_0, for which the prey is most effective. Similarly, we assume that the predator death rate d depends upon v and is minimum at the trait value v_0, at which predator are best adapted to their environment. Finally, we assume that the predation rate is a function of both traits, and that predator [prey] are favoured [unfavoured] when traits are balanced, i.e. when u and v are in a

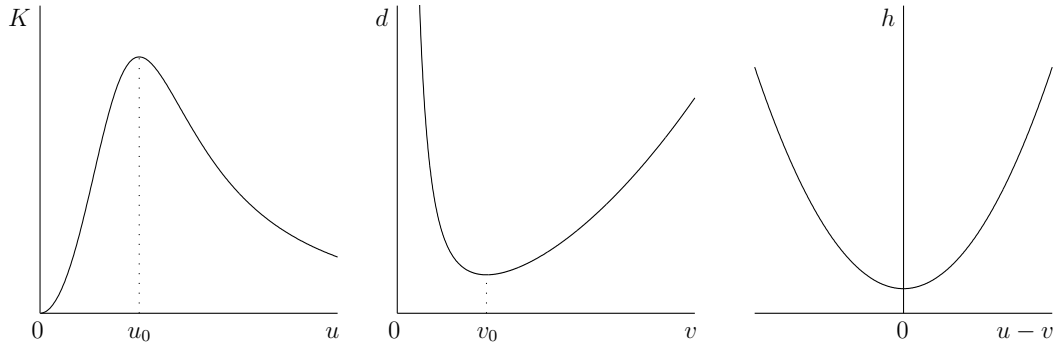

Figure A3: Dependence of the parameters K, d and h upon the prey's and predator's adaptive traits u and v.

suitable relationship, which defines the so-called bidirectional axis of prey vulnerability (Abrams, 2000). This mechanism is present if, for example, the searching effectiveness of the predator depends upon both traits but with a certain degree of plasticity, so that the same effectiveness can be achieved for a continuum of pairs (u, v). Since the half saturation constant h is inversely related to searching effectiveness, the result is that the function $h(u, v)$ is minimum when u and v are balanced. For notational convenience we assume that the traits are measured on a scale such that they balance for $u = v$. In conclusion, we will concentrate on the dependence of the following triplet of demographic parameters upon the traits

$$K = K(u) \quad d = d(v) \quad h = h(u, v) \tag{A9}$$

where K is maximum at u_0, d is minimum at v_0, and h is minimum both with respect to u and v for $u = v$. Our assumption on the relationships between traits and demographic parameters is by no means more meaningful than others from a biological point of view. However, it has the advantage of involving the minimum possible number of demographic parameters. The functions K, d and h used in the following for performing simulations and bifurcation analyses are (see Fig. A3):

$$K(u) = K_0 \frac{2}{\left(\frac{u}{u_0}\right)^2 + \left(\frac{u_0}{u}\right)^2} \quad d(v) = d_0 \frac{\left(\frac{v}{v_0}\right)^2 + \left(\frac{v_0}{v}\right)^2}{2} \quad h(u, v) = h_0 + h_1(u - v)^2 \tag{A10}$$

(eq. (5) in paper). Although these functions do not have a specific empirical underpinning, they satisfy all the requirements we have just discussed, they are smooth and can be easily changed by varying their parameters (two for each function).

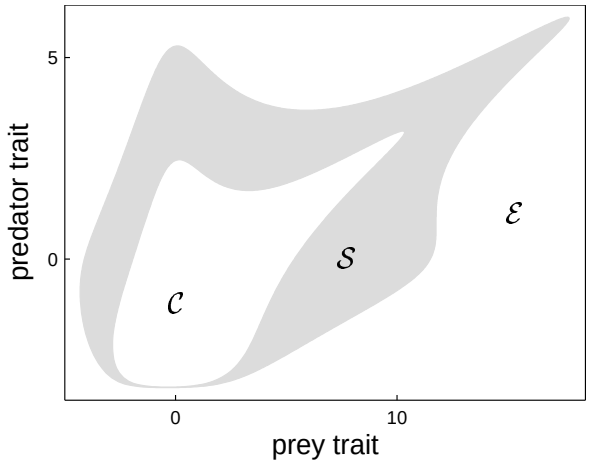

Figure A4: Regions $\mathcal{E}$, $\mathcal{S}$ (grey region), and $\mathcal{C}$, in the trait space (u, v); for $(u, v) \in \mathcal{E}$ the predator population goes extinct (see eq. (A3) and Fig. A1A); for $(u, v) \in \mathcal{S}$ the attractor of model (A1, A2) is an equilibrium (stationary coexistence, see eq. (A4) and Fig. A1B); for $(u, v) \in \mathcal{C}$ the attractor is a limit cycle (cyclic coexistence, see eq. (A6) and Fig. A1C); the figure has been obtained for the following parameter setting: $K_0 = 1$, $h_0 = 0.02$, $h_1 = 0.02$, $d_0 = 0.01$, $b = 0.001$, $ea = 0.5$, $u_0 = 1$, $v_0 = 3$.

A4 Regions of stationary and cyclic coexistence in trait space

Given the possible asymptotic regimes of model (A1, A2), we can immediately infer that the space (u, v) of the traits can be partitioned into three regions $\mathcal{E}$, $\mathcal{S}$, and $\mathcal{C}$ characterised by inequalities (A3), (A4), and (A6), respectively. For traits in region $\mathcal{E}$ the predator population can not persist on ecological timescale, while for traits in regions $\mathcal{S}$ (called stationary coexistence region) and $\mathcal{C}$ (called cyclic coexistence region) the populations persist in stationary or cyclic conditions, respectively. Fig. A4 shows an example of the three regions for the particular parameter setting indicated in the caption. For other parameter settings some of these three regions can disappear or become unbounded. Notice that a nonlinear transformation of the traits appear on the axis of Fig. A4, under which the point (u_0, v_0) becomes the origin.

At the boundary separating region $\mathcal{S}$ from region $\mathcal{C}$ all quantities associated with the asymptotic regime of the slow-fast system are discontinuous. In fact, close to the boundary in region $\mathcal{S}$ the vertical predator isocline is on the right of the vertex of the prey isocline but close to it. Thus, the asymptotic regime is stationary and the equilibrium $(\bar{x}, \bar{y})$ given by eq. (A5) is characterised by a value of $\bar{y}$ very close to $y_{\max}$. By contrast, for pairs (u, v) close to the boundary in region $\mathcal{C}$ the attractor of the slow-fast system is well approximated by the singular limit cycle shown in Fig. A2 which is characterised by a mean value of the predator population much lower than $y_{\max}$ (De Feo and Rinaldi, 1997). This means that an abrupt loss of the mean predator population will accompany any evolutionary transition from region $\mathcal{S}$ to region $\mathcal{C}$, while

a sharp increase will occur when evolution proceeds in the opposite direction. Notice that these results are correct for the limit case of complete timescale separation of prey and predator ecological dynamics. However, singular perturbation theory (Tikhonov, 1952; Hoppensteadt, 1966, 1974) guarantees that for the general and more realistic case of contrasting (but not separated) timescales, the evolutionary transition from $\mathcal{S}$ to $\mathcal{C}$, though formally continuous, will be associated with a sharp and marked loss of mean predator population.

A5 The the canonical equation of adaptive dynamics

In order to obtain a set of two coupled autonomous ODEs describing the dynamics of the two traits, we follow the approach of adaptive dynamics, centred on the assumption that random mutations are small and occur rarely (Metz et al., 1996; Dieckmann and Law, 1996; Geritz et al., 1997, 1998). This means that the prey [predator] resident population with density x [y] and trait u [v] generates, from time to time, a small mutant population x' [y'] with trait u' [v'] slightly different from u [v]. After the mutation has occurred, the system is composed of three populations, two of which, namely the resident x [y] and the mutant x' [y'] are in competition. If the mutant population does not invade, the trait u' [v'] is ruled out from the game, while in the opposite case the mutant population grows, at least temporarily. The possibility of a temporary growth of the mutant population followed by its extinction can be excluded in our case, because this would require the existence of multiple attractors of the population model (Dercole et al., 2002), while model (A1, A2) has a single attractor. Thus, only the fate of the resident population after invasion of the mutant remains to be established. In general, this is not always easy to settle. It might be that the resident goes extinct, so that the mutant replaces the former resident and the trait u [v] is replaced, in the end, by u' [v']. But it might also be that the resident and the mutant populations achieve stationary or cyclic coexistence. For large classes of models (in particular Lotka-Volterra models), both stationary and cyclic coexistence can be excluded, but in other models coexistence is possible. In our case, if the mutant is the predator, we have two predator populations (the resident and the mutant) competing exploitatively for the same (logistic) resource. Two predators and one prey can coexist on a limit cycle (Koch, 1974; Hsu et al., 1978), but the conditions for cyclic coexistence in the case of slow predator and fast prey are not satisfied if mutations are small (Muratori and Rinaldi, 1989). Therefore, we can conclude that an invading predator replaces the former resident. Finally, as far as prey mutations are concerned, the so-called invasion implies substitution principle (see Dercole and Rinaldi, 2006) generically guarantees that, if the resident populations are at ecological equilibria, an invading prey mutant substitutes the resident population. Thus, if successful mutations are

small and occur rarely enough, evolutionary dynamics within each population remain monomorphic and are described by the so-called canonical equation of adaptive dynamics (Dieckmann and Law, 1996):

$$\dot{u} = k^u \langle x \rangle \langle s^u \rangle \tag{A11}$$

$$\dot{v} = k^v \left\langle \left(b + \frac{eax}{h+x} \right) y \right\rangle \left\langle \frac{s^v}{b + \frac{eax}{h+x}} \right\rangle \tag{A12}$$

(eqs. (6) and (7) in paper), where k^u and k^v are parameters proportional to the probability of mutation in the prey and predator resident populations, and s^u and s^v, called selection derivatives, are the derivatives with respect to mutant's trait of the initial per-capita rate of increase of the prey and predator mutant populations.

In order to transform eqs. (A11, A12) into autonomous ODEs one must first determine the selection derivatives s^u and s^v. After a mutation has occurred in the prey, the resident-mutant model is:

$$\begin{aligned}
\dot{x} &= rx \left(1 - \frac{x}{K(u)} - \frac{x'}{K(u)} C(u,u') \right) - \frac{A(u,v)x}{1 + A(u,v)Hx + A(u',v)Hx'} y \\
\dot{x}' &= rx' \left(1 - \frac{x}{K(u')} C(u',u) - \frac{x'}{K(u')} \right) - \frac{A(u',v)x'}{1 + A(u,v)Hx + A(u',v)Hx'} y \\
\dot{y} &= y \left(b + e \frac{A(u,v)x + A(u',v)x'}{1 + A(u,v)Hx + A(u',v)Hx'} - d(v) \right)
\end{aligned} \tag{A13}$$

where $C(u,u')$ describes prey intra-specific competition ($C(u,u) = 1$) (MacArthur, 1969, 1970; Gatto, 1990), and $A(u,v)$ and H are predator attack rate and handling time, respectively. Using attack rate A and handling time H, instead of maximum predation rate a and half-saturation constant h, is useful for writing the type II functional response when more than one type of prey is available to the predator (Murdoch, 1969; Chesson, 1983). In the case of a single type of prey $A = a/h$ and $H = 1/a$. We assume symmetric intra-specific competition (i.e. $C(u,u') = C(u',u)$) and, in particular, that $C(u,u')$ is an even function of the difference $u - u'$. Analogously, after the mutation has occurred in the predator population, the resident-mutant model is:

$$\begin{aligned}
\dot{x} &= rx \left(1 - \frac{x}{K(u)} \right) - \frac{ax}{h(u,v) + x} y - \frac{ax}{h(u,v') + x} y' \\
\dot{y} &= y \left(b + e \frac{ax}{h(u,v) + x} - d(v) \right) \\
\dot{y}' &= y' \left(b + e \frac{ax}{h(u,v') + x} - d(v') \right)
\end{aligned} \tag{A14}$$

The prey and predator selection derivatives are therefore given by

$$\begin{aligned} s^u &= \frac{\partial}{\partial u'}\left(\frac{\dot{x}'}{x}\right)\Big|_{\substack{u'=u\\x'=0}} = \frac{r}{K^2}K_u x + a\frac{h_v}{h}\frac{y}{h+x} \\ s^v &= \frac{\partial}{\partial v'}\left(\frac{\dot{y}'}{y}\right)\Big|_{\substack{v'=v\\y'=0}} = -eah_v\frac{x}{(h+x)^2} - d_v \end{aligned} \tag{A15}$$

Notice that due to the above assumptions on the competition function C, its first-order derivative does not appear in the selection derivative for the prey.

In conclusion, equations (A11) and (A12) can be given the form

$$\dot{u} = k^u \langle f_1 \rangle \left(\frac{r}{K^2}K_u \langle f_1 \rangle + a\frac{h_u}{h}\langle f_2 \rangle\right) \tag{A16}$$

$$\dot{v} = k^v d \langle f_3 \rangle \left(-d_v \langle f_4 \rangle - eah_v \langle f_5 \rangle\right) \tag{A17}$$

where K_u, d_v, h_u, h_v are the derivatives with respect to u and v of the triplet K, d, h given by eq. (A10) and $\langle f_i \rangle$, $i = 1,\ldots,5$, are the average values on the population attractor corresponding to traits (u, v) of the functions

$$f_1 = x \quad f_2 = \frac{y}{h+x} \quad f_3 = y \quad f_4 = \frac{h+x}{bh+(ea+b)x} \quad f_5 = \frac{x}{(ea+b)x^2 + h(ea+2b)x + bh^2} \tag{A18}$$

Exceptions to monomorphic evolutionary dynamics can occur through prey evolutionary branching (Geritz et al., 1997, 1998) only when traits reach an evolutionary equilibrium of the canonical equation (A11, A12). Prey evolutionary branching has been studied in Dercole et al. (2003) but will not be investigated here.

A6 Derivation of the canonical equation in the stationary coexistence region

Each term $\langle f_i \rangle$ in (A18) can be computed in the region of stationary coexistence, i.e. for $(u, v) \in \mathcal{S}$, by replacing x and y with their equilibrium values given by eq. (A5). After some algebra one obtains

$$\langle f_1 \rangle = \frac{h(d-b)}{ea-d+b} \tag{A19}$$

$$\langle f_2 \rangle = \frac{r}{a}\left(1 - \frac{h}{K}\frac{d-b}{ea-d+b}\right) \tag{A20}$$

$$\langle f_3\rangle = \frac{rh}{a}\left(1-\frac{h}{K}\frac{d-b}{ea-d+b}\right)\left(1+\frac{d-b}{ea-d+b}\right) \tag{A21}$$

$$\langle f_4\rangle = \frac{1}{d} \tag{A22}$$

$$\langle f_5\rangle = \frac{(d-b)(ea-d+b)}{hde^2a^2} \tag{A23}$$

Thus, the canonical equation in region $\mathcal{S}$ is composed of eqs. (A10, A16, A17, A19–A23).

A7 Derivation of the canonical equation in the cyclic coexistence region

The terms $\langle f_i\rangle$ in the region of cyclic coexistence, i.e. for $(u,v)\in\mathcal{C}$, can be computed through a series of approximations. The computation is performed under the assumption that the prey population has fast dynamics in comparison with the predator population, and that the half-saturation constant is small with respect to the carrying capacity of the prey, i.e. $h/K \ll 1$. Thus, $\langle f_i\rangle$ can be identified with the average value of f_i on the singular limit cycle (see Fig. A2). Since this cycle is composed of two slow and two fast segments, the computation can be limited to the slow segments. More precisely, if the duration of the first slow phase (along the y axis) is T' and the duration of the second slow phase (along the parabola) is T'', we can write

$$\langle f_i\rangle = \frac{1}{T'+T''}\left(\int_0^{T'} f_i\,dt + \int_0^{T''} f_i\,dt\right)$$

where the two integrals are computed along the slow segments of the singular cycle.

Computation of T' and T''

The first slow phase of the singular cycle is characterised by $y(0)=y_{\max}$ and $x(t)=0$, so that $\dot y=(b-d)y$, i.e. $y(t)=y_{\max}\exp(b-d)t$. Since $y(T')=y_{\min}$, we obtain

$$T' = \frac{1}{d-b}\log\frac{y_{\max}}{y_{\min}} \tag{A24}$$

where $y_{\max}$ is given by (A7) and $y_{\min}$ is identified by (A8).

The second slow phase of the singular cycle is characterised by $x\gg h$, since $h\ll K$. Hence, eq. (A2) can be approximated by $\dot y=(b+ea-d)y$ which has the solution $y(t)=y_{\min}\exp(b+ea-d)t$, since $y(0)=y_{\min}$. Since $y(T'')=y_{\max}$, we obtain

$$T'' = \frac{1}{ea-d+b}\log\frac{y_{\max}}{y_{\min}} \tag{A25}$$

Computation of $\langle f_1 \rangle$

During the first slow phase of the singular limit cycle the function f_1 is zero (see eq. (A18)). This implies that

$$\langle f_1 \rangle = \frac{1}{T' + T''} \int_0^{T''} x(t)\, dt$$

where the integration must be performed along the parabola, where

$$x(t) = \frac{K-h}{2} + \frac{K}{2}\sqrt{\left(a + \frac{h}{K}\right)^2 - \frac{4a}{rK} y(t)} \tag{A26}$$

$$y(t) = y_{\min} \exp(ea - d + b)t \tag{A27}$$

This integration can be performed explicitly, without introducing any further approximation. Taking eqs. (A24, A25) into account, the result is eq. (A28), with β, γ and the function Φ as in (A33).

Computation of $\langle f_2 \rangle$

From eq. (A18), we can write

$$\langle f_2 \rangle = \frac{1}{T' + T''} \left(\frac{1}{h} \int_0^{T'} y(t)\, dt + \int_0^{T''} \frac{y(t)}{h + x(t)}\, dt \right)$$

In the first integral $y(t) = y_{\max} \exp(b - d)t$, while in the second integral $x(t)$ and $y(t)$ are as in eqs. (A26, A27). If h is neglected with respect to x in the second term, the two integrals can be performed analytically and the result, using eq. (A24, A25), is equation (A29), with α as in (A33).

Computation of $\langle f_3 \rangle$

From eq. (A18) it follows that

$$\langle f_3 \rangle = \frac{1}{T' + T''} \left(\int_0^{T'} y(t)\, dt + \int_0^{T''} y(t)\, dt \right)$$

where in the first integral $y(t) = y_{\max} \exp(b - d)t$, while in the second integral $y(t)$ can be approximated by the exponential function (A27). A straightforward integration gives eq. (A30).

Computation of $\langle f_4 \rangle$

During the first slow phase of the singular limit cycle, f_4 is constant and equal to $1/b$, while during the second slow phase it is approximately constant and equal to $1/(ea+b)$ (see eq. (A18)). Thus,

$$\langle f_4 \rangle = \frac{T'}{T'+T''}\frac{1}{b} + \frac{T''}{T'+T''}\frac{1}{ea+b}$$

from which, taking eq. (A24, A25) into account, eq. (A31) follows.

Computation of $\langle f_5 \rangle$

During the first slow phase of the singular limit cycle, f_5 is zero, while it can be approximated with $1/((ea+b)x)$ during the second slow phase (see eq. (A18)). Hence,

$$\langle f_5 \rangle = \frac{1}{T'+T''}\int_0^{T''} \frac{1}{x(t)}\,dt$$

where $x(t)$ is given by eq. (A26) with $y(t)$ as in eq. (A27). Also this integral can be computed, using classical decomposition techniques, and the result is eq. (A32).

Computation of $y_{\min}$

The extreme values $y_{\max}$ and $y_{\min}$ of predator density along the singular limit cycle are given by eqs. (A7, A8). While eq. (A7) defines $y_{\max}$ explicitly, eq. (A8) is a transcendental equation that can be solved with respect to $y_{\min}$ only numerically. In order to avoid such a computation each time the right-hand side of the canonical equation must be evaluated for different parameter and trait values, we use an approximated formula for $y_{\min}$, obtained by neglecting the terms of order higher than two in the Taylor's expansion

$$\exp\frac{y_{\min}}{y_0} = 1 + \frac{y_{\min}}{y_0} + \frac{1}{2}\left(\frac{y_{\min}}{y_0}\right)^2 + O\left(\left(\frac{y_{\min}}{y_0}\right)^3\right)$$

The corresponding approximated, but explicit, formula for $(y_{\max} - y_{\min})$ is given in eq. (A33). Of course, the approximation is good if $y_{\min} \ll y_0$, which can be shown to be always the case for $h \ll K$.

Validity of the approximations

All the approximations we have introduced are a priori justified if $h \ll K$. In order to evaluate to which extent our approximations are valid we have systematically compared the values of $\langle f_i \rangle$, $i = 1, \ldots, 5$, given

by eq. (A28–A33), with the true values computed through numerical integration of the function f_i along the singular cycle. The result of this analysis, carried out for many parameter settings, is that the approximation is definitely satisfactory for $\langle f_2\rangle$,..., $\langle f_5\rangle$ (errors of the order of 1% if $h/K \leq 0.2$). By contrast, the approximation of $\langle f_1\rangle$ is more crude but still acceptable ($\leq 1\%$ for $h/K \leq 0.1$). Of course, in order to be sure that the impact of our approximations on the final results is not too heavy we should look at the values of h/K in region $\mathcal{C}$. For this, we can first notice that for a particularly meaningful pair of traits, namely the optimal pair (u_0, v_0), h/K is simply given by (see eq. (A10))

$$\frac{h}{K} = \frac{h_0 + h_1(u_0 - v_0)^2}{K_0}$$

and that this value is definitely low (between 0.05 and 0.1 and exceptionally 0.2) in all the examples considered in the paper. A more meaningful indicator is perhaps the portion of region $\mathcal{C}$ in which $h/K \leq 0.2$. Computed on our state portraits this indicator is quite satisfactory: at 95% of the points $(u, v) \in \mathcal{C}$ the ratio h/K is lower than 0.2.

Conclusions

In conclusion, the final result of our analysis is the following

$$\langle f_1\rangle = \frac{K(d-b)}{2ea}\left\{\alpha + \frac{hr}{a}\frac{\beta\left[\Phi(-\beta) - \Phi(\beta)\right] - 2\gamma}{y_{\max} - y_{\min}}\right\} \tag{A28}$$

$$\langle f_2\rangle = \frac{r(ea - d + b)}{ea^2} + \frac{hr^2(d-b)}{ea^3(y_{\max} - y_{\min})}\left[\gamma + \alpha\Phi(\alpha)\right] \tag{A29}$$

$$\langle f_3\rangle = \frac{hr}{a} \tag{A30}$$

$$\langle f_4\rangle = \frac{ea - d + 2b}{b(ea + b)} \tag{A31}$$

$$\langle f_5\rangle = \frac{r(d-b)}{ea^2(y_{\max} - y_{\min})(ea + b)}\left[\alpha\Phi(\alpha) + \frac{h}{K}\Phi(-\beta) - \Phi(\beta)\right] \tag{A32}$$

where α, β, γ, and the functions Φ and $(y_{\max} - y_{\min})$ are given by

$$\alpha = 1 - \frac{h}{K} \quad \beta = 1 + \frac{h}{K} \quad \gamma = \sqrt{\frac{4a}{rK}(y_{\max} - y_{\min})} \quad \Phi(w) = \log \frac{w}{\gamma + w}$$
$$y_{\max} - y_{\min} = \frac{r(h+K)^2}{4aK} - \frac{hr}{a}(\rho - \sqrt{\rho^2 - 2}) \quad \rho = \frac{\exp\left(\dfrac{(h+K)^2}{4hK}\right)}{\dfrac{(h+K)^2}{4hK}} - 1 \tag{A33}$$

To sum up, the canonical equation in region $\mathcal{C}$ is approximated by eqs. (A10, A16, A17, A28–A33).

A8 Bifurcation analysis of the canonical equation

The canonical equation (A16, A17) is formally a discontinuous piecewise smooth autonomous dynamical system, also called *Filippov system* (Filippov, 1964, 1988), namely a set of ODEs whose right-hand side is smooth in regions $\mathcal{S}$ (see eqs. (A19–A23)) and $\mathcal{C}$ (eqs. (A28–A33)), but discontinuous at the boundary between them. This discontinuity is the origin of the novel phenomena of evolutionary sliding and pseudo-equilibria. Details on the definition and computation of sliding motions can be found in Filippov (1988) who has been the leading authority in this field since the early sixties.

The most obvious way of studying the canonical equation (A16, A17) is through simulation. For this, after fixing the parameter values, one must simply specify the ancestral conditions, namely the initial values of the traits $(u(0), v(0))$ in the region of coexistence $\mathcal{S} \cup \mathcal{C}$, and then integrate forward in time. The trajectory starting at $(u(0), v(0))$ tends either toward region $\mathcal{E}$, thus revealing a case of predator evolutionary extinction, or toward an attractor in the region of stationary and/or cyclic coexistence. If the ancestral conditions are changed, a new evolutionary path is obtained and the fate of the two populations along this path might be different from the previous one because the canonical equation, being nonlinear, can have multiple attractors. Repeating this process for a sufficiently high number of initial conditions, one obtains a state portrait, namely a set of trajectories in the space (u, v) that fully describes the dynamics of the traits. Moreover, if the two coexistence regions $\mathcal{S}$ and $\mathcal{C}$ are reported in the same diagram, then basic qualitative informations on population dynamics can also be identified.

In order to keep the number of simulations under control and still arrive to some meaningful conclusion about the influence of various parameters on the eco-evolutionary dynamics, one is forced to study the canonical equation, at least to a certain extent, through bifurcation analysis (Kuznetsov, 1998). This means that all the invariant sets of the state portrait (e.g. equilibria and limit cycles, as well as pseudo-equilibria

and sliding segments) must be “continued” with respect to a parameter by means of some suitable software (we used SlideCont (Dercole and Kuznetsov, 2005), Auto (Doedel et al., 1997), and Content (Kuznetsov and Levitin, 1997)), in order to detect the critical values of the parameter at which they undergo a bifurcation, i.e. a structural change.

The bifurcation analysis of the canonical equation is much more complex than that of a standard dynamical system, because Filippov systems, besides having all standard bifurcations, have also special bifurcations involving some sliding on the discontinuity boundary (for this reason called *sliding bifurcations*). The simplest example is the appearance or disappearance of a sliding segment, a structural change which can be continued with respect to two parameters. In other words, the points in a two parameter space associated with the appearance of a sliding segment lie on a curve that can be produced through numerical continuation. Another example of sliding bifurcation is the collision of an equilibrium with the discontinuity boundary. Under suitable conditions, this bifurcation gives rise to a pseudo-equilibrium.

The list of the sliding bifurcations is very long and actually known only in the special case of second order systems (Kuznetsov et al., 2003). The use of numerical bifurcation analysis is really mandatory, because the bifurcations and attractors involved in our study are far too many to allow one to reach a useful synthesis only through simulation. However, the presentation of the bifurcation analysis is out of the scope of the present paper. It would require a deep knowledge of sliding bifurcations, a topic that has only recently been touched in the literature.

References

Abrams, P. A. 2000. The evolution of predator-prey interactions: Theory and evidence. Annual Review of Ecology and Systematics 31:79–105.

Chesson, J. 1983. The estimation and analysis of preference and its relationship to foraging models. Ecology 64:1297–1304.

De Feo, O., and Rinaldi, S. 1997. Yield and dynamics of tritrophic food chains. The American Naturalist 150:328–345.

Dercole, F., and Kuznetsov, Yu. A. 2005. Slidecont: An Auto97 driver for bifurcation analysis of Filippov systems. ACM Transactions on Mathematical Software 31:95–119.

Dercole, F., and Rinaldi, S. 2006. Analysis of Evolutionary Processes: The Adaptive Dynamics Approach and its Applications. Princeton University Press. (forthcoming).

Dercole, F., Ferrière, R., and Rinaldi, S. 2002. Ecological bistability and evolutionary reversals under asymmetrical competition. Evolution 56:1081–1090.

Dercole, F., Irisson, J.-O., and Rinaldi, S. 2003. Bifurcation analysis of a prey-predator coevolution model. SIAM Journal on Applied Mathematics 63:1378–1391.

Dieckmann, U., and Law, R. 1996. The dynamical theory of coevolution: A derivation from stochastic ecological processes. Journal of Mathematical Biology 34:579–612.

Doedel, E., Champneys, A., Fairgrieve, T., Kuznetsov, Yu. A., Sandstede, B., and Wang, X. 1997. AUTO97: Continuation and bifurcation software for ordinary differential equations (with HOMCONT). Department of Computer Science, Concordia University, Montreal, QC.

Filippov, A. F. 1964. Differential equations with discontinuous right-hand side. In *American Mathematical Society Translations, Series 2*, pages 199–231. American Mathematical Society.

—. 1988. Differential Equations with Discontinuous Righthand Sides. Kluwer Academic Publishers, Dordrecht.

Gatto, M. 1990. A general minimum principle for competing populations: Some ecological and evolutionary consequences. Theoretical Population Biology 37:369–388.

Geritz, S. A. H., Metz, J. A. J., Kisdi, E., and Meszéna, G. 1997. The dynamics of adaptation and evolutionary branching. Physical Review Letters 78:2024–2027.

Geritz, S. A. H., Kisdi, E., Meszéna, G., and Metz, J. A. J. 1998. Evolutionarily singular strategies and the adaptive growth and branching of the evolutionary tree. Evolutionary Ecology 12:35–57.

Hoppensteadt, F. 1966. Singular perturbations on the infinite interval. Transactions of the American Mathematical Society 123:521–535.

—. 1974. Asymptotic stability in singular perturbation problems. Journal of Differential Equations 15:501–521.

Hsu, S. B., Hubbel, S. P., and Waltman, P. A. 1978. A contribution to the theory of competing predators. Ecological Monographs 48:337–349.

Koch, A. L. 1974. Competitive coexistence of two predators utilizing the same prey under constant environmental conditions. Journal of Theoretical Biology 44:387–395.

Kuznetsov, Yu. A. 1998. Elements of Applied Bifurcation Theory. Springer Verlag, Berlin, second edition.

Kuznetsov, Yu. A., and Levitin, V. V. 1997. CONTENT: A multiplatform environment for analyzing dynamical systems. Dynamical Systems Laboratory, Centrum voor Wiskunde en Informatica, Amsterdam, The Netherlands available from `ftp.cwi.nl/pub/CONTENT`.

Kuznetsov, Yu. A., Rinaldi, S., and Gragnani, A. 2003. One parameter bifurcations in planar Filippov systems. International Journal of Bifurcation and Chaos 13:2157–2188.

MacArthur, R. H. 1969. Species packing, and what interspecies competition minimizes. Proceedings of the National Academy of Sciences USA 64:1369–1371.

—. 1970. Species packing and competitive equilibrium for many species. Theoretical Population Biology 1:1–11.

Metz, J. A. J., Geritz, S. A. H., Meszéna, G., Jacobs, F. J. A., and van Heerwaarden, J. S. 1996. Adaptive dynamics: A geometrical study of the consequences of nearly faithful reproduction. In S. J. van Strien and S. M. Verduyn Lunel, eds., *Stochastic and Spatial Structures of Dynamical Systems*, pages 183–231. Elsevier Science, North-Holland, Amsterdam.

Muratori, S., and Rinaldi, S. 1989. Remarks on competitive coexistence. SIAM Journal on Applied Mathematics 49:1462–1472.

Murdoch, W. W. 1969. Switching in general predators: experiments on prey specificity and stability of prey populations. Ecological Monographs 39:335–354.

Rinaldi, S., and Muratori, S. 1992. Slow-fast limit cycle in predator-prey models. Ecological Modelling 61:287–308.

Rosenzweig, M. L., and MacArthur, R. H. 1963. Graphical representation and stability conditions of predator-prey interactions. The American Naturalist 97:209–223.

Tikhonov, A. M. 1952. Systems of differential equations containing small parameters at derivatives. Matematicheskii Sbornik, Moscow 31:575–586. (in Russian).